RESEARCH ARTICLE

ORGANIC SYNTHESIS

An oxidative photocyclization approach to the synthesis of *Securiflustra securifrons* alkaloids

Brandon W. Alexander[1]†, Noah M. Bartfield[1]†, Vaani Gupta[1], Brandon Q. Mercado[1,2], Mark Del Campo[3], Seth B. Herzon[1,4,5]*

Securines and securamines are cytotoxic alkaloids that contain reactive alkene and heterocyclic residues embedded in skeletons comprising four to six oxidized rings. This structural complexity imparts a rich chemistry to the isolates but has impeded synthetic access to the structures in the nearly three decades since their isolation. We present a flexible route to eight isolates that exemplify the three skeletal classes of metabolites. The route proceeds by the modular assembly of the advanced azides 38 and 49 (13 steps, 6 to 10% yield), sequential oxidative photocyclizations, and late-stage functional group manipulations. With this approach, the targets were obtained in 17 to 19 steps, 12 to 13 purifications, and 0.5 to 3.5% overall yield. The structure of an advanced intermediate was elucidated by microcrystal electron diffraction (MicroED) analysis. The route will support structure-function and target identification studies of the securamines.

Bryozoa are a rich source of structurally diverse halogenated secondary metabolites (*1*). In 1996, Christophersen and coworkers reported the characterization of securamines A (**1**) and B (**2**) in extracts of the bryozoan *Securiflustra securifrons* (Fig. 1A) (*2*). Subsequently, the cytotoxic hexacyclic bis(aminal) isolates securamines D (**3**) and C (**4**) and related isolates that differ in the oxidation state at the C2–C3 linkage [such as securamine G (**5**)] or the halogenation pattern on the indoline [such as securamine I (**6**)] were discovered (*3*–*5*). Despite their relatively small structures, these alkaloids present major challenges to chemical synthesis, including an unstable *cis*-enamide, a neopentylic secondary alkyl chloride, a basic haloimidazole, and a labile halogenated indoline residue. Since the 1990s, numerous groups have worked toward the synthesis of securamines (*6*–*10*) and the related chartellines (*11*–*24*). As a testament to the challenges posed by their structures, securamines have yet to be prepared through chemical synthesis, with the synthesis of chartelline C (**9**) (Fig. 1B) reported by Baran and Shenvi in 2006 (*13*, *16*) standing as the only completed route to any isolate structurally related to **1** to **8**. These prior studies make clear that the close proximity of reactive functional groups leads to unexpected reactivity, rendering well-designed approaches to the isolates unfeasible. Further highlighting their complex reactivity, Christophersen reported the reversible, solvent-dependent isomerization of securamines A (**1**) and B (**2**) to the macrolactam-indole derivatives securines A (**7**) and B (**8**) (*2*). Hansen observed the reversible incorporation of methanol at the C2 position of the extended Michael acceptor within hexacyclic isolates and reported that their cellular toxicity increases with increasing pyrroloindoline halogenation (*4*). Collectively, these observations suggest that the indoline halogenation and electrophilic character at C2 cooperatively enhance activity, but the mechanism of action and intracellular target of the molecules is not known.

In prior studies toward chartelline C (**9**), Baran and Nishikawa (*13*, *16*, *24*) constructed the spirocyclic β-lactam through sequential indole oxidation at C20 and rearrangement of an aza-*ortho*-quinone methide intermediate (**10**) (Fig. 1B) (*25*). This approach may mimic the biosynthesis of chartelline C (**9**). 2,3-Disubstituted indoles are known to react with singlet (*26*) and triplet (*27*) dioxygen to form 3-hydroperoxyindolenines, which may convert to an aza-*ortho*-quinone methide after addition of N1 to C12 (Fig. 1C). In reconciling the putative biosynthesis of chartelline C (**9**) and the hexacyclic securamines **3** to **6**, which bear an unusual oxidized urea residue, we took note of studies examining the photooxidation of simple imidazoles (*28*) and histidine residues in proteins (*29*) with singlet dioxygen. Foundational studies by Wasserman (*30*, *31*) and Foote (*32*) established that addition of singlet dioxygen to imidazole provides an *endo*-peroxide that undergoes ring-opening to the electrophilic acylimine **11** (Fig. 1D). In biological systems, singlet dioxygen can be formed enzymatically or through energy transfer from photoexcited aromatic amino acids, porphyrins, or aromatic hydrocarbons (*33*). These data suggest to us that the reported ring closure (*2*) of securines A (**7**) and B (**8**) to their respective securamines (**1** and **2**, respectively) could mask the reactive indole residue and divert oxidation toward the bromoimidazole, providing securamines D (**3**) and C (**4**) (Fig. 1E). Although the photooxidation of 2-haloimidazoles is not known, one can envision a mechanism that comprises photocycloaddition to form the endoperoxide **12**, cyclization by C8–N13 bond formation, and collapse of the 2,3-dioxa-5,7-diazabicyclo[2.2.1]heptane intermediate **13**.

Synthetic strategy

We envisioned that N^5-benzyloxymethyl (BOM) securamine A (**14**) might serve as a common precursor to the three distinct isolates shown in Fig. 1A and that **14** could be derived from the isomeric α,β-unsaturated γ-lactam **15** through a cycloisomerization (*34*, *35*). The α,β-unsaturated γ-lactam **15** was prepared by means of acid-mediated chlorination and skeletal remodeling of the 12-membered macrolactam **16**, followed by reduction of the nitroarene. The macrolactam was traced to a convergent assembly of the β-ketophosphonate **17**, the aldehyde **18**, and iodoacetamide (**19**). This strategy avoids introduction of the reactive pyrroloindoline residue until late in the sequence and installation of the chloride functionality by an invertive displacement, which had hindered prior studies (*8*, *10*). Additionally, macrocycle **16** might serve a strategic role in controlling enamide geometry, and by varying the ketophosphonate **17** and carrying out late-stage peripheral modifications, this route could be adapted to the synthesis of securamines C (**4**), G (**5**), or I (**6**).

Synthesis of a precursor to securamine A (1) and securine A (7)

Our synthesis of the aldehyde **18** builds on studies toward chartelline C (**9**) by Weinreb and coworkers (Fig. 2A) (*17*). Treatment of (4-imidazolyl)acetonitrile (**20**) with sodium hydride and benzyl chloromethyl ether (BOMCl) provided a mixture of N1 and N3 benzyloxymethyl ether derivatives [~1:2 ratio of N1 and N3 alkylation; proton nuclear magnetic resonance (^{1}H NMR) analysis]. This mixture was isomerized to the more stable N1-benzyloxymethyl isomer **21** by heating with substoichiometric amounts of benzyloxymethyl chloride (0.10 equiv; single regioisomer by means of ^{1}H NMR analysis; 60 to 80% from **20**) (*36*). Twofold methylation of **21** (potassium *tert*-butoxide, iodomethane, 18-crown-6) provided the α-quaternary nitrile **22** (94%, 6.5 g scale). The C5-bromoimidazole **23** was obtained through site-selective bromination (*17*) of **22** by using benzyltrimethylammonium

[1]Department of Chemistry, Yale University, New Haven, CT 06511, USA. [2]Chemical and Biological Instrumentation Center, Yale University, New Haven, CT 06511, USA. [3]Rigaku Americas Corporation, The Woodlands, TX 77381, USA. [4]Department of Pharmacology, Yale School of Medicine, New Haven, CT 06510, USA. [5]Department of Therapeutic Radiology, Yale School of Medicine, New Haven, CT 06510, USA.
*Corresponding author. Email: seth.herzon@yale.edu
†These authors contributed equally to this work.

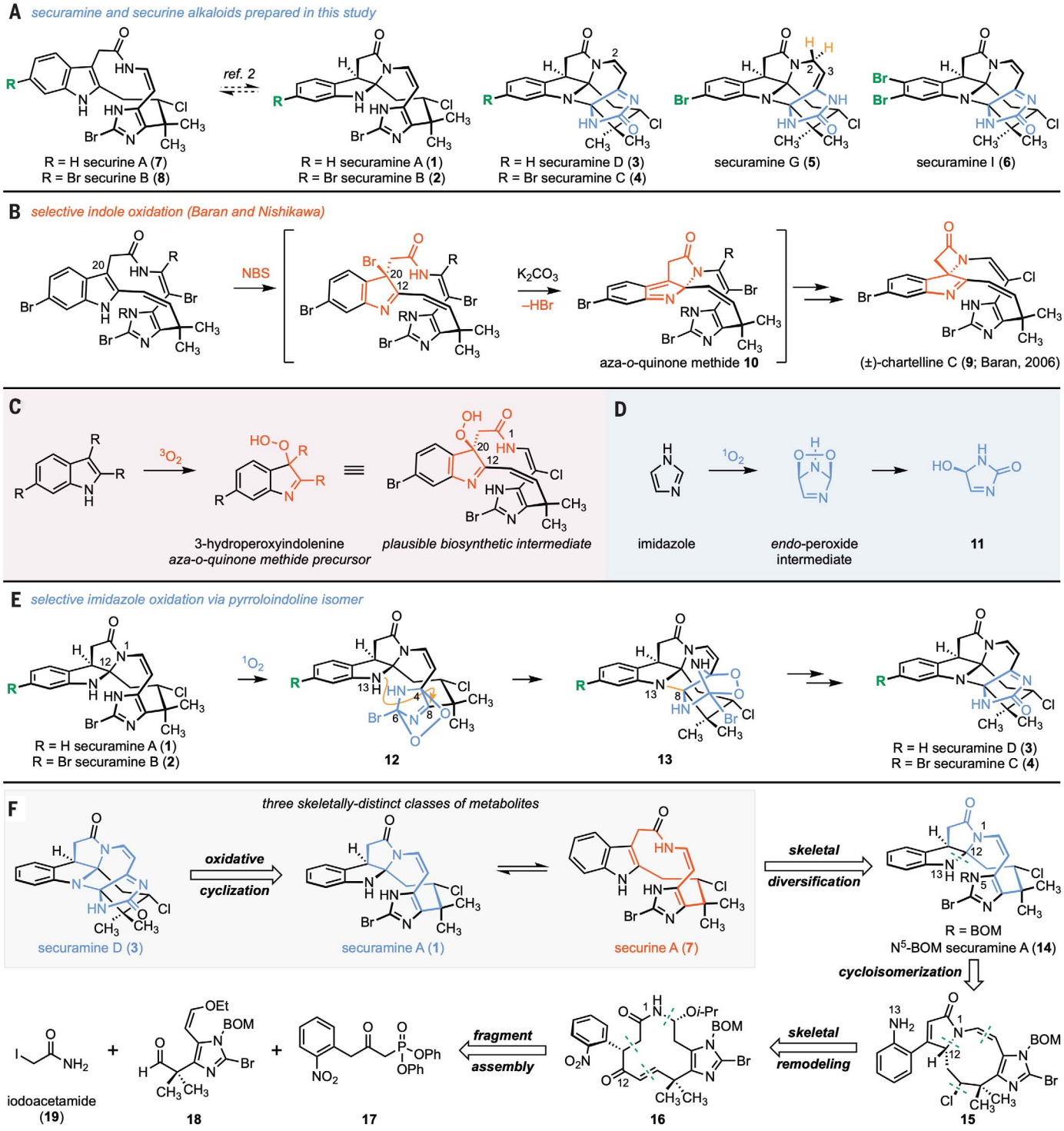

Fig. 1. Background and synthetic plan. (**A**) Structures of securamines A to D (**1**, **2**, **4**, and **3**, respectively), securamine G (**5**), securamine I (**6**), and securines A and B (**7** and **8**, respectively). (**B**) Oxidative rearrangement approach to the construction of the spirocyclic β-lactam within chartelline C (**9**). (**C**) The addition of dioxygen to 2,3-disubstituted indoles provides 3-hydroperoxyindolenines. This oxidation may occur in the biosynthesis of chartelline C (**9**). (**D**) Intermediates in the oxidation of imidazole with singlet dioxygen. (**E**) Postulated selective imidazole oxidation of securamines A (**1**) and B (**2**) to form hexacyclic securamines D (**3**) and C (**4**). (**F**) Synthetic strategy for the assembly of N^5-BOM securamine A (**14**), a potential precursor to securamine A (**1**), securine A (**7**), and securamine D (**3**).

tribromide (69%, 2.0 g scale). Stille cross-coupling with *cis*-1,2-ethoxytributylstannane (**24**) provided the enol ether **25** as a single detectable *cis*-diastereomer (^{1}H NMR analysis; 92%, 3.9 g scale). Deprotonation of the C2 position [lithium diisopropyl amide (LDA); 3.3 g scale] followed by addition of tetrabromomethane furnished a C2-bromoimidazole. Reduction of the nitrile by use of chlorobis(cyclopentadienyl)-hydridozirconium (Schwartz's reagent) (*37*) then formed the aldehyde **18** (87%, from **25**; 41% from **20**).

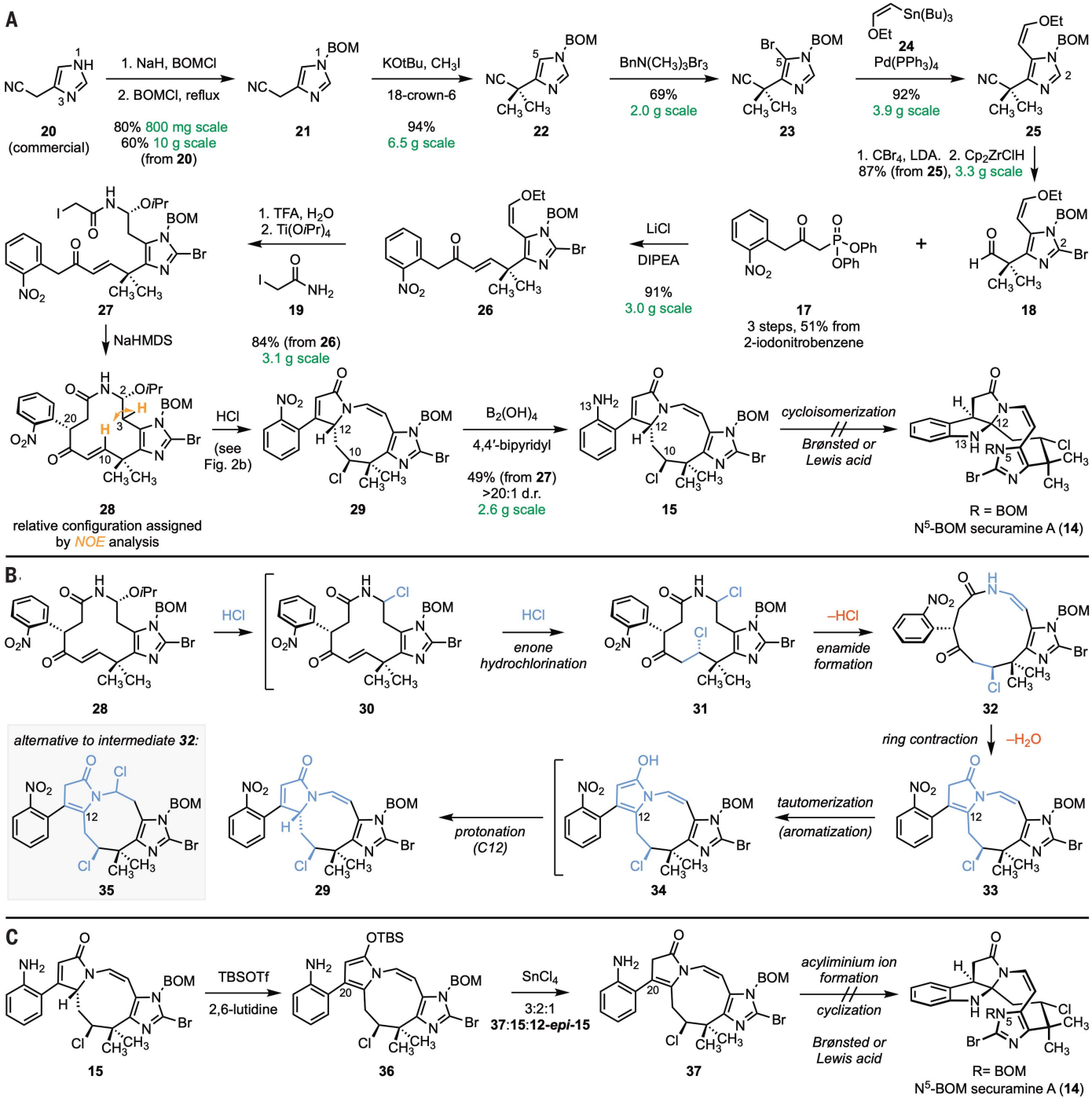

Fig. 2. Synthesis of a precursor to securamine A (1) and securine A (7). (**A**) Synthesis of the α,β-unsaturated-γ-lactam **15**, an isomer of N^5-BOM securamine A (**14**). The synthetic route provides **15** as a racemate; the (*10S*, *12R*) enantiomer is arbitrarily depicted. (**B**) Mechanistic proposal for the transformation of **28** to **29**, based on LC-MS monitoring of the reaction at 0°C (fig. S2). (**C**) Synthesis of the β,γ-unsaturated-γ-lactam **37** and attempted isomerization to N^5-BOM securamine A (**14**).

The β-keto phosphonate **17** was prepared in three steps and 51% yield from 2-iodonitrobenzene (supplementary materials). Fragment coupling of **17** and the aldehyde **18** under Masamune–Roush olefination conditions [lithium chloride and diisopropylethylamine (DIPEA)] (*38*) provided the α,β-unsaturated ketone **26** as a single detectable (*E*)-diastereomer (^{1}H NMR analysis; 91%, 3.0 g scale). Hydrolysis of the enol ether [trifluoroacetic acid (TFA) and water] followed by addition of iodoacetamide (**19**) to the resulting aldehyde (titanium isopropoxide) formed the racemic macrocyclization precursor **27** (84%, two steps, 3.1 g scale). Base-mediated cyclization of **27** [sodium hexamethyldisilazide (NaHMDS), 1.10 equiv] generated the macrolactam **28** as a 19:1 mixture of diastereomers. The relative configuration of the C2 and C20 centers was assigned by nuclear Overhauser effect (NOE) analysis in conjugation with molecular dynamics simulations (fig. S1).

In a critical transformation that involves remodeling of nearly every functional group in the 12-membered macrolactam **28**, dissolution of **28** in anhydrous hydrochloric acid–dioxane (4.0 M) at 23°C was found to provide the chlorinated 1-aza-bicyclo[7.3.0]dodec-2,10-diene **29** as a single detectable diastereomer (^{1}H NMR analysis). When this reaction was carried out in a mixture of toluene and dioxane at 0°C, the reaction rate was diminished, and the intermediates in the transformation could be identified with liquid chromatography–mass spectrometry (LC-MS) analysis (Fig. 2B and fig. S2). These studies suggest initial substitution of the *iso*-propoxy substituent provided

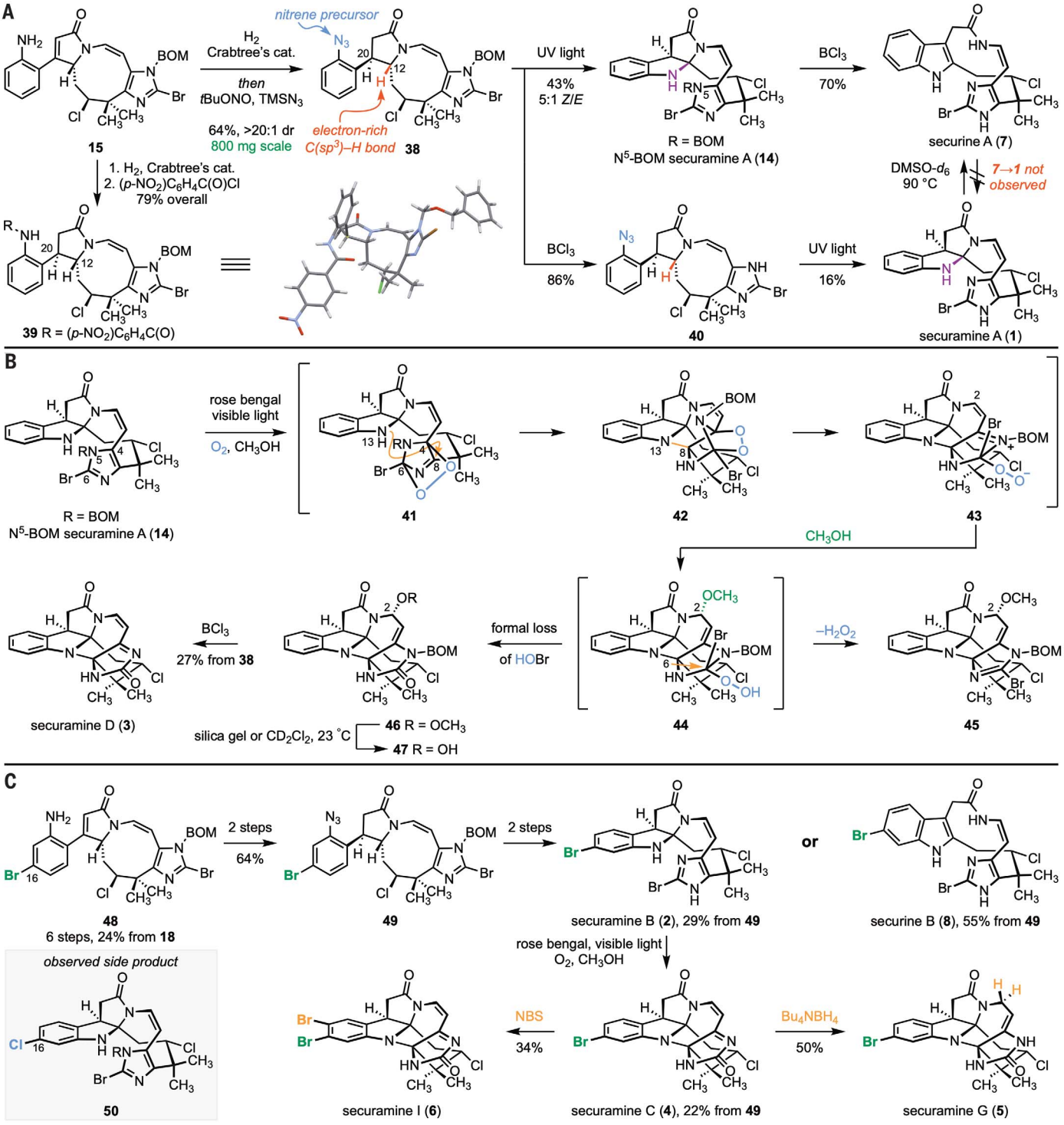

Fig. 3. Completion of the synthesis of the securamine A (1), securine A (7), and adaptation of the route to other securamines and securines. (**A**) Synthesis of the *N*-aryl azide **38** and its elaboration to securamine A (**1**) and securine A (**7**). MicroED analysis of the acetanilide **39** served to confirm the connectivity and stereochemical assignment of **38**. (**B**) Photooxidation of N^5-BOM securamine A (**14**) and elaboration of the photooxidation product **46** to securamine D (**3**). (**C**) Synthesis of securamines B (**2**), C (**4**), G (**5**), and I (**6**) and securine B (**8**). The chloride **50** was identified as a side product when the photochemical reaction of **49** was conducted in dichloromethane.

the *N*-acyl chloroaminal **30**, which was observed as the corresponding hemiaminal in LC-MS analysis. Enone hydrochlorination (**30**→**31**) was followed by elimination to the enamide (**31**→**32**) and ring contraction to provide the β,γ-unsaturated-γ-lactam **33**. Tautomerization to the hydroxypyrrole **34** and protonation at C12 provided the observed product **29**. On the basis of the available data, an alternate sequence proceeding through **35** instead of **32** cannot be excluded. This cascade reaction forms the *cis*-enamide, neopentylic alkyl chloride, γ-lactam, and a nine-membered ring—four challenging substructures present in the securamines—in a single step.

Selective reduction of the nitroarene in the presence of other reducible functionalities was achieved by treating the lactam **29** with tetrahydroxydiboron and 4,4′-bipyridine (*39*) to provide the complex lactam **15**. Because intermediates **28** and **29** were difficult to obtain in analytically pure form, we advanced them without purification in preparative-scale experiments. By this approach, the lactam **15** was obtained in three steps and 49% yield from **27** (>20:1 diastereomeric ratio, ^{1}H NMR analysis; 2.6 g scale).

We envisioned that isomerization of the lactam **15** to an *N*-acyliminium ion, followed by ring closure (N13–C12 bond formation), would provide N^5-BOM securamine A (**14**). However, we were unable to actualize this strategy, potentially because of the basicity of the imidazole and/or aniline. To circumvent this, we developed a two-step procedure to obtain the alternative *N*-acyliminium precursor **37** (Fig. 2C). Treatment of the aniline **15** with *tert*-butyldimethylsilyl trifluoromethanesulfonate (TBSOTf) and 2,6-lutidine provided the siloxypyrrole **36**. Exposure of **36** to tin tetrachloride (*40*) at –78°C generated a 3:2:1 mixture of the β,γ-unsaturated-γ-lactam **37**, **15**, and ***12-epi*-15**. Unfortunately, all attempts to induce cyclization of **37** by using Lewis or Brønsted acids [such as mercury(II) acetate or trifluoroacetic acid] resulted in reversion to **15**. Additionally, we noted that ***12-epi*-15** spontaneously isomerized to **15** upon standing in dichloromethane-d_2 at 23°C, suggesting that **15** is the thermodynamically favored stereoisomer. We presume that this epimerization proceeds through an aromatic hydroxypyrrole analogous to that of **34** (Fig. 2B).

Completion of the synthesis by photochemical nitrene insertion

Drawing inspiration from recent advances in the photochemistry of *N*-aryl azides (*41*–*43*) and the insertion of *N*-aryl nitrenes into aliphatic C–H bonds (*44*, *45*), we conceived a strategy to access the *cis*-fused pyrroloindoline framework by forming the N13–C12 bond through C–H amination (Fig. 3A). For this transformation to be feasible, the C12–H bond and *N*-aryl nitrene must reside on the same face of the lactam, which would require a facially selective reduction of the unsaturated γ-lactam **15**. A single diastereomer (^{1}H NMR analysis) of the hydrogenation product was obtained when **15** was treated with Crabtree's catalyst [(tricyclohexylphosphine)(1,5-cyclooctadiene)(pyridine)iridium(I) hexafluorophosphate] and dihydrogen (*46*). Acylation of the hydrogenation product with 4-nitrobenzoyl chloride provided the acetanilide **39** (79% overall). Although NMR analysis suggested that the reduction proceeded with the desired stereoselectivity ($^3J_{H12–20}$ ~ 0 Hz), we carried out many attempts to obtain single crystals of **39** to confirm this assignment with x-ray analysis. However, the compound presented as thin, microcrystalline platelets unsuitable for conventional crystallography. Accordingly, we turned to microcrystal electron diffraction (MicroED) (*47*, *48*), which confirmed that the acetanilide **39** possessed the relative configuration required for the proposed C–H amination (fig. S3). Our MicroED studies also revealed that the BOM ether populated four conformers in the solid state, which explains our inability to grow uniform single crystals of **39** (figs. S4 and S5).

The azide **38** was prepared by means of sequential hydrogenation of **15** and exposure to *tert*-butyl nitrite (*t*BuONO) and trimethylsilyl azide ($TMSN_3$; 64% from **15**, 800 mg scale). Irradiation of solutions of **38** in dichloromethane with ultraviolet (UV) light (medium-pressure Hg lamp, 100 W, borosilicate filter) provided N^5-BOM securamine A (**14**) as a 5:1 mixture of (*Z*)- and (*E*)-enamide diastereomers (43%). Removal of the BOM ether (boron trichloride) proceeded with concomitant opening of the pyrroloindoline to the indole, affording securine A (**7**, 70%; 17 steps, 12 purifications, 3.0% overall). NMR spectroscopic data for natural and synthetic securine A (**7**) in dimethyl sulfoxide-d_6 (DMSO-d_6) were in agreement (table S1) (*2*). However, whereas Christophersen reported that dissolution of natural securine A (**7**) in chloroform-*d* induced isomerization to securamine A (**1**) (*2*), we observed line broadening and no evidence of the pyrroloindoline framework (fig. S6). We reasoned that the solvent used might have contained acidic impurities (*2*), but we did not observe isomerization when phosphoric, trifluoroacetic, or hydrochloric acid were added to the NMR sample (fig. S6).

Fortunately, we were able to obtain securamine A (**1**) by reordering the steps in the sequence. Treatment of the azide **38** with boron trichloride provided the NH imidazole **40** (86%). Irradiation of **40** with UV light then generated securamine A (**1**; 16%; 17 steps, 12 purifications, 1.4% overall). The diminished yield of this transformation relative to **38**→**14** (43%) points toward the free imidazole in **40**, which may divert the nitrene from productive C–H insertion through nucleophilic trapping. Spectroscopic data for synthetic and natural securamine A (**1**) in chloroform-*d* were in agreement (table S2). Solutions of synthetic securamine A (**1**) were indefinitely stable at 23°C in DMSO-d_6, which contradicts Christophersen's observations (*2*). However, upon warming to 90°C, we did observe near-quantitative isomerization to securine A (**7**). Consistent with our experimental findings, density functional theory (DFT) calculations (optimized geometries and computational details are provided in fig. S7) indicate that securamine A (**1**) is >4 kcal/mol less stable than securine A (**7**) (corresponding to an equilibrium ratio of **7**:**1** of >10^3). Collectively, our data suggest that securamine A (**1**) is kinetically stable and that the ring-opening to securine A (**7**) is irreversible.

Synthesis of additional securines and securamines

Our route to N^5-BOM securamine A (**14**) enabled us to investigate photooxidation and conversion to securamine D (**3**) (Fig. 3B). We found that irradiation of mixtures of rose bengal and N^5-BOM securamine A (**14**) in methanol under an atmosphere of dioxygen provided a 1:1.6 mixture (^{1}H NMR analysis) of the amidinyl bromide **45** (tentatively assigned) and the imidazolone **46**. Both products were found to incorporate methanol at C2, in accord with the reactivity recorded earlier by Hansen and coworkers (*4*). Because the methyl ether within **46** underwent substitution by water (**46**→**47**) to varying extents during NMR analysis and purification, the mixture of **45** and **46** was treated directly with boron trichloride in dichloromethane to provide securamine D (**3**; 27% from **38**; 18 steps, 12 purifications, 2.7% overall). NMR spectroscopic data for synthetic and natural securamine D (**3**) in chloroform-*d* were in agreement (table S3) (*2*). The photoxidation of 2-haloimidazoles is apparently unknown, and several mechanistic pathways for the transformation of N^5-BOM securamine A (**14**) to **45** and **46** can be envisioned. For example, [4+2] cycloaddition to form the endoperoxide **41**, cyclization to the intermediate **42** (C8–N13 bond formation), fragmentation of the peroxyaminal to the extended iminium ion **43**, and addition of methanol would provide the C6 tetrahedral intermediate **44**. This intermediate could partition between the observed products **46** and **45** through formal loss of hypobromous acid or hydrogen peroxide, respectively.

Modification of the arene in the β-ketophosphonate **17** was anticipated to provide access to additional securamines (Fig. 3C). To illustrate this, we synthesized the C16-bromoaniline **48** in six steps and 24% yield from the aldehyde **18** (supplementary materials). Although the absolute stereochemistry of the securamines is not known, optical rotations have been reported for all isolates. We developed a method to efficiently

resolve the aniline (±)-**48** by acylation with (*S*)-(−)-fluorenylethylchloroformate (FLEC-Cl) on preparative scales (fig. S8) (*49*). This resolution provides a path to establish the absolute configuration of a broad range of isolates. Analogous to the securamine A (**1**) series, the C16-bromoaniline **48** was converted to the azide **49** by reduction and diazotransfer (64% overall) (Fig. 3C). Securamine B (**2**) was obtained by removing the benzyloxymethyl ether protecting group (boron trichloride) and C–H amination (medium-pressure Hg lamp, 100 W, borosilicate filter; 29% from **49**; 17 steps, 12 purifications, 1.8% overall). Alternatively, the sequence of C–H amination followed by protecting group removal provided securine B (**8**; 55% from **49**; 17 steps, 12 purifications, 3.5% overall). When these C–H amination reactions were carried out in dichloromethane, we observed minor amounts of aryl chloride **50**, potentially arising from homolysis of the C16–Br bond and abstraction of chloride from solvent. Fortunately, this was suppressed by using dibromomethane as solvent. Spectroscopic data for natural and synthetic securamine B (**2**) and securine B (**8**) were in agreement (tables S4 and S5).

Direct photooxidation of securamine B (**2**) (rose bengal and methanol) provided securamine C (**4**, 22% from **48**; 18 steps, 12 purifications, 1.4% overall). The reported propensity of the oxidized securamine scaffolds to act as a Michael acceptor (*4*) under ambient conditions motivated us to consider the conjugate reduction of securamine C (**4**) to provide securamine G (**5**) (*3*). Addition of tetrabutylammonium borohydride (Bu_4NBH_4) to solutions of securamine C (**4**) in dichloromethane generated securamine G (**5**, 50%; 19 steps, 13 purifications, 0.7% overall). Alternatively, bromination of securamine C (**4**) [*N*-bromosuccinimide (NBS)] provided securamine I (**6**, 34%; 19 steps, 13 purifications, 0.5% overall) (*4*). Natural securamine C (**4**) (*2*), G (**5**) (*3*), and I (**6**) (*4*) were characterized in chloroform-*d*, but we found that synthetic samples of these compounds were insoluble in chloroform-*d* (fig. S9). It seems plausible that the presence of variable amounts of methanol, water, and other organic impurities in samples of natural securamines C (**4**) and I (**6**) may have promoted their dissolution in chloroform-*d* (*4*). Graphical reproductions of NMR spectra for securamines A (**1**), B (**2**), and G (**5**) and securines A and B (**7** and **8**), are not available (*2*, *3*). We therefore characterized them in DMSO-d_6 (tables S6 to S8). We obtained natural securamine I (**6**) and found that it was identical to synthetic material by means of NMR analysis in DMSO-d_6 and with LC-MS co-injection (figs. S10 to S12 and table S8).

Conclusions

We devised synthetic routes to eight isolates representing the three skeletal classes in securamines and securines. The hydrochlorination cascade (**28**→**29**) (Fig. 2A) we discovered installs many of the challenging functional groups in the targets in a single step while also achieving a productive remodeling of the skeletal framework of our intermediates. Sequential photochemical C–H amination and cycloaddition of singlet dioxygen enabled rapid access to the pyrroloindoline residue and hexacyclic scaffold of the targets. The success of the selective oxidation of the bromoimidazole residue lends support to the hypothesis that divergent biosynthetic oxidations of the indole-bearing securines and masked-indole securamines lead to skeletally distinct metabolites. Although we cannot recapitulate the previously reported securamine-securine equilibrium (*2*), our data make clear that synthetic samples of securines do not readily interconvert with their pyrroloindoline counterparts. Fortunately, the photochemical C–H amination we developed allowed us to circumvent this unexpected challenge. Pyrroloindolines are widespread in secondary metabolites (*50*), and we anticipate that this amination approach will be of general utility in accessing this substructure. This study also underscores the utility of MicroED as an indispensable tool for complex molecule structure determination.

REFERENCES AND NOTES

1. M. L. Ciavatta *et al*., *Mar. Drugs* **18**, 200 (2020).
2. L. Rahbaek, U. Anthoni, C. Christophersen, P. H. Nielsen, B. O. Petersen, *J. Org. Chem.* **61**, 887–889 (1996).
3. L. Rahbæk, C.Christophersen, *J. Nat. Prod.* **60**, 175–177 (1997).
4. K. Ø. Hansen *et al*., *J. Nat. Prod.* **80**, 3276–3283 (2017).
5. K. Ø. Hansen *et al*., *Nat. Prod. Commun.* **16**, 1934578X2199618 (2021).
6. S. C. Chaffee, "Synthetic studies toward the securamine alkaloids," thesis, Yale University (2001).
7. P. Korakas, "Progress toward the total synthesis of securamine A: Construction of the securamine macrocyclic core," thesis, Yale University (2004).
8. P. Korakas, S. Chaffee, J. B. Shotwell, P. Duque, J. L. Wood, *Proc. Natl. Acad. Sci. U.S.A.* **101**, 12054–12057 (2004).
9. P. Aggarwal, "Studies directed toward total synthesis of securine A and securamine A," thesis, Penn State Univeristy (2007).
10. S. Kikuchi, "Studies toward the biomimetic synthesis of marine alkaloids," thesis, Harvard University (2011).
11. P. E. Murray, "Approaches to the synthesis of the marine alkaloid chartellamide A: A novel 2-(4-imidazoly)indole," thesis, The University of Manchester (1998).
12. X. Lin, "Part one: Generation and cyclization of nitrogen radicals. Application to a formal total synthesis of (+/−)-peduncularine. Part two: Studies towards the total synthesis of chartelline A," thesis, Pennsylvania State University (2002).
13. P. S. Baran, R. A. Shenvi, C. A. Mitsos, *Angew. Chem. Int. Ed.* **44**, 3714–3717 (2005).
14. J. M. Rohde, "Synthetic approaches to aplydactone and chartellamide A inspired by biosynthetic hypotheses," thesis, Scripps Research Institute (2005).
15. C. Sun, "Chapter one: Stereoselective total synthesis of the racemic and natural enantiomer of the marine tunicate alkaloid lepadiformine. Chapter two: Studies directed towards a total synthesis of chartelline A," thesis, Pennsylvania State University (2005).
16. P. S. Baran, R. A. Shenvi, *J. Am. Chem. Soc.* **128**, 14028–14029 (2006).
17. C. Sun, X. Lin, S. M. Weinreb, *J. Org. Chem.* **71**, 3159–3166 (2006).
18. P. J. Black, E. A. Hecker, P. Magnus, *Tetrahedron Lett.* **48**, 6364–6367 (2007).
19. J. E. Camp, "Chapter one: Studies directed towards a total synthesis of the chartellamides. Chapter two: Studies directed towards a total synthesis of the chartellines," thesis, Pennsylvania State University (2008).
20. E. A. Hecker, "Studies toward the total synthesis of (±)-chartelline C and (−)-platensimycin," thesis, University of Texas at Austin (2008).
21. S. Kajii, T. Nishikawa, M. Isobe, *Chem. Commun.* (27): 3121–3123 (2008).
22. R. A. Shenvi, "Pure and applied science in the chemical syntheses of marine alkaloids chartelline C and cortistatin A," thesis, Scripps Research Institute (2008).
23. K. Iwasaki *et al*., *Angew. Chem. Int. Ed.* **51**, 9160–9163 (2012).
24. Y. Nakane, A. Nakazaki, T. Nishikawa, *J. Org. Chem.* **85**, 7534–7542 (2020).
25. H.-H. Liao, S. Miñoza, S.-C. Lee, M. Rueping, *Chem. Eur. J.* **28**, e202201112 (2022).
26. I. Saito, T. Matsuura, M. Nakagawa, T. Hino, *Acc. Chem. Res.* **10**, 346–352 (1977).
27. T. Hino, M. Nakagawa, *Heterocycles* **8**, 743 (1977).
28. M. R. Iesce, F. Cermola, F. Temussi, *Curr. Org. Chem.* **9**, 109–139 (2005).
29. L. Grassi, C. Cabrele, *Amino Acids* **51**, 1409–1431 (2019).
30. H. H. Wasserman, K. Stiller, M. B. Floyd, *Tetrahedron Lett.* **9**, 3277–3280 (1968).
31. H. H. Wasserman, M. S. Wolff, K. Stiller, I. Saito, J. E. Pickett, *Tetrahedron* **37**, 191–200 (1981).
32. P. Kang, C. S. Foote, *J. Am. Chem. Soc.* **124**, 9629–9638 (2002).
33. M. J. Davies, *Biochem. Biophys. Res. Commun.* **305**, 761–770 (2003).
34. F. Souquet *et al*., *Synthesis* **52**, 2970 (2020).
35. A. Umehara, H. Ueda, H. Tokuyama, *Tetrahedron* **79**, 131809 (2021).
36. Y. He, Y. Chen, H. Du, L. A. Schmid, C. J. Lovely, *Tetrahedron Lett.* **45**, 5529–5532 (2004).
37. M. M. Więcław, S. Stecko, *Eur. J. Org. Chem.* **2018**, 6601–6623 (2018).
38. M. A. Blanchette *et al*., *Tetrahedron Lett.* **25**, 2183–2186 (1984).
39. M. Jang, T. Lim, B. Y. Park, M. S. Han, *J. Org. Chem.* **87**, 910–919 (2022).
40. N. Langlois, P. K. Choudhury, *Tetrahedron Lett.* **40**, 2525–2528 (1999).
41. S. C. Patel, N. Z. Burns, *J. Am. Chem. Soc.* **144**, 17797–17802 (2022).
42. D. A. Davydov, M. A. Giricheva, Y. B. Malysheva, G. K. Fukin, A. V. Budruev, *J. Org. Chem.* **88**, 14998–15006 (2023).
43. T. J. Pearson *et al*., *Science* **381**, 1474–1479 (2023).
44. B. C. G. Soderberg, *Curr. Org. Chem.* **4**, 727–764 (2000).
45. T. G. Driver, *Org. Biomol. Chem.* **8**, 3831–3846 (2010).
46. R. H. Crabtree, M. W. Davis, *J. Org. Chem.* **51**, 2655–2661 (1986).
47. T. Gruene *et al*., *Angew. Chem. Int. Ed.* **57**, 16313–16317 (2018).
48. C. G. Jones *et al*., *ACS Cent. Sci.* **4**, 1587–1592 (2018).
49. S. Einarsson, B. Josefsson, P. Möller, D. Sanchez, *Anal. Chem.* **59**, 1191–1195 (1987).
50. P. Ruiz-Sanchis, S. A. Savina, F. Albericio, M. Álvarez, *Chemistry* **17**, 1388–1408 (2011).

ACKNOWLEDGMENTS

We thank K. Hansen (Marbio, UiT The Arctic University of Norway) for kindly providing a sample of natural securamine I (**6**) and for helpful discussions. We thank S. Ohlinger (Wavefunction) for assistance with calculations. **Funding:** Financial support from the National Science Foundation (CHE-1954319 and Graduate Research Fellowship to N.M.B.) is gratefully acknowledged. **Author contributions:** B.W.A., N.M.B., and V.G. carried out the experimental work. B.Q.M and M.D.C. carried out MicroED analysis of **39**. B.W.A., N.M.B., V.G., and S.B.H. wrote the manuscript. S.B.H. directed the study. **Competing interests:** None. **Data and materials availability:** Crystallographic data for **39** has been deposited in the Cambridge Crystallographic Data Centre (CCDC# 2294680). **License information:** Copyright © 2024 the authors, some rights reserved; exclusive licensee American Association for the Advancement of Science. No claim to original US government works. https://www.science.org/about/science-licenses-journal-article-reuse

SUPPLEMENTARY MATERIALS

science.org/doi/10.1126/science.adl6163
Materials and Methods
Supplementary Text
Figs. S1 to S12
Tables S1 to S14
References (*51*–*70*)
Data S1

Submitted 27 October 2023; accepted 22 January 2024
10.1126/science.adl6163